BIOCHEMISTRY
including biophysical chemistry & molecular biology

Article

pubs.acs.org/biochemistry

Directed Evolution of a Probe Ligase with Activity in the Secretory Pathway and Application to Imaging Intercellular Protein−Protein Interactions

Katharine A. White*,† and Phillip M. Zegelbone‡

Department of Chemistry, Massachusetts Institute of Technology, 77 Massachusetts Avenue, Cambridge, Massachusetts 02139, United States

Supporting Information

ABSTRACT: Previously, we reported a new method for intracellular protein labeling in living cells called PRIME (probe incorporation mediated by enzymes). PRIME uses a mutant of *Escherichia coli* lipoic acid ligase (LplA) to catalyze covalent probe ligation onto a 13-amino acid peptide recognition sequence. While our first demonstration labeled proteins with a coumarin fluorophore, subsequent engineering produced alkyl azide and *trans*-cyclooctene ligases as well as an interaction-dependent form of the coumarin PRIME method (ID-PRIME). One major limitation of the PRIME methodologies is that LplA mutants have very low activity in the secretory pathway. Here, we extend PRIME labeling to oxidizing compartments such as the endoplasmic reticulum and the cell surface. We used yeast-display evolution and four rounds of selection to isolate LplA mutants with improved picolyl azide ligation activity. Then we compared the ligation activities of the evolved mutants both *in vitro* and on the mammalian cell surface. We characterized the picolyl azide ligation activity of the most active LplA variant *in vitro*, in the endoplasmic reticulum, and at the mammalian cell surface. Finally, we used the optimized LplA variant to label neurexin and neuroligin interactions at the mammalian cell surface in just 5 min. Compared to another method for imaging these protein−protein interactions (GFP recomplementation across synapses), our optimized ID-PRIME ligase is faster, more sensitive, and does not trap interacting proteins in a complex (nontrapping).

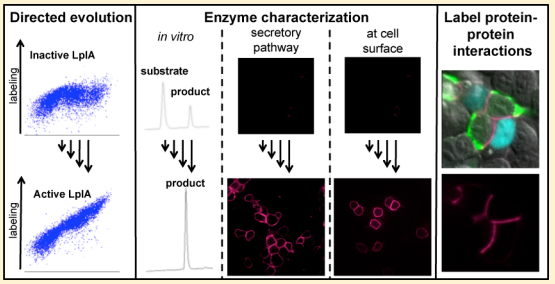

Probe incorporation mediated by enzymes (PRIME) is a methodology for site-specific protein labeling that utilizes mutants of *Escherichia coli* lipoic acid ligase (LplA) to catalyze covalent probe ligation to a 13-amino acid LplA acceptor peptide (LAP). We have used engineered LplA to label both intracellular[1,2] and cell-surface proteins with a wide variety of probes.[3−5] The recent extension of the PRIME methodology to interaction-dependent labeling (ID-PRIME)[6] expanded the range of biological problems that can be studied with this method. However, a major limitation of PRIME is that LplA and its mutants have low activity in the secretory pathway[1] and when expressed on the cell surface. This limitation excludes PRIME from a host of biological applications for which it is particularly suited, such as utilizing the compartmentalized labeling technology to monitor receptor trafficking, labeling protein−protein interactions in the endoplasmic reticulum, and interactions at the neuronal synapse.

In an attempt to improve LplA activity along the secretory pathway, we put considerable effort into the rational engineering of the enzyme. LplA has six surface cysteines, all of which are reduced in the native form of the protein, with disulfide-induced inactivation of LplA previously reported.[7] We hypothesized that the oxidizing environment of the secretory pathway was inducing intra- or intermolecular disulfide formation, resulting in misfolding or inactivation of LplA. To test this theory, we made a series of rationally designed LplA mutants in which the cysteine residues were mutated to serines. However, we found that these mutations did not improve the activity of LplA in the secretory pathway (data not shown). This demonstrates that while rational design can be a valuable tool for enzyme engineering, it often requires extensive knowledge of the functional, structural, and mechanistic properties of an enzyme. Directed enzyme evolution, on the other hand, does not require *a priori* knowledge of a protein's properties to produce desired characteristics.

Directed evolution can be a powerful technique for altering existing properties of enzymes or producing new enzyme function.[8,9] However, there are significant technological limitations to the types of enzymatic reactions that can be selected. For example, high-throughput enzyme library screening in multiwell plates has been frequently used for enzyme evolution when chromogenic or fluorogenic substrates were available.[10] One significant drawback to using these screening techniques is that enzyme library sizes are limited to 10^2−10^6 members and the evolution of novel activity has proven to be intractable. *In vivo* selections have also been used to produce

Received: March 2, 2013
Revised: April 12, 2013
Published: April 24, 2013

improved enzyme activity;[11,12] however, these techniques are limited to selection for specific reporter genes, and controlling selection conditions inside living cells can be difficult.[13] Phage display, mRNA display, and ribosome display have been used to produce enzymes with improved activities[14,15] and altered specificities.[16,17] These display methods allow for exquisite control over selection conditions and accommodate larger library sizes (up to 10^{13}).[18] However, designing selections for these techniques that appropriately link phenotype (enzymatic product) and genotype (DNA) is challenging.[19]

Yeast and bacterial cell-surface display have emerged as powerful and generalizable directed evolution methods[20−22] with numerous benefits. First, unlike other display methods, cell-surface display allows one copy of a gene to produce up to 10^5 copies of the library member for display.[21,22] Second, fluorescence-activated cell sorting can be used in phenotype selection strategies. Third, because the enzyme is displayed on the cell surface, selection conditions are more controllable than when using other cell-based selections. For our purposes, yeast display is an ideal evolution platform because all library members are trafficked through the endoplasmic reticulum for display.

In this work, we describe the *in vitro* directed evolution of a PRIME ligase with improved ligation activity *in vitro*, in the secretory pathway, and on the cell surface. First, we describe the yeast display of an LplA enzyme library and selection for LplA variants with improved picolyl azide (pAz) ligation activity. Second, we present the characterization of the isolated LplA variants *in vitro*, on the surface of yeast and mammalian cells, and in the endoplasmic reticulum of mammalian cells. Third, we demonstrate how the optimized pAz ligase can be applied in labeling intercellular neurexin and neuroligin interactions on live cells. Finally, we compare this new method of ID-PRIME to a commonly used split-GFP technique called GFP recomplementation across synaptic partners (GRASP).

EXPERIMENTAL PROCEDURES

Lipoylation on the Yeast Cell Surface (Figure 1B). See general yeast methods in the Supporting Information for details on yeast protocols and recipes for media. *Saccharomyces cerevisiae* cells constitutively displaying the LAP peptide (LAP-YIP yeast) and inducibly displaying ^{WT}LplA or ^{W37A}LplA were pelleted and washed twice with phosphate-buffered saline (PBS, pH 7.5) with 1 mg/mL bovine serum albumin (PBS-B). Cells were resuspended to a cell density of 2×10^8 cells/mL in PBS-B with 500 μM lipoic acid, 5 mM $Mg(OAc)_2$, and 3 mM ATP and incubated on a rotator at 30 °C for 1−3 h. The reactions were stopped by pelleting the cells and washing them with ice-cold PBS-B containing 100 mM EDTA. Cells were washed an additional time with ice-cold PBS-B. The ligated lipoic acid was detected using rabbit polyclonal anti-lipoic acid antibody (Calbiochem), and the LplA surface expression level was detected using mouse monoclonal anti-HA antibody (Roche) in PBS-B at 1:200 dilutions. Cells were incubated with the primary antibodies for 40 min on a rotator at 4 °C. Cells were pelleted and washed twice with ice-cold PBS-B. Then the yeast cells were incubated with anti-rabbit R-phycoerythrin (PE) (Invitrogen) and anti-mouse AlexaFluor-488 secondary antibodies (AF488) (Invitrogen) in PBS-B at 1:100 dilutions for 40 min on a rotator at 4 °C. Cells were pelleted and washed twice with ice-cold PBS-B and then resuspended in PBS-B to a density of $\sim 1 \times 10^7$ cells/mL for fluorescence-activated cell sorting (FACS).

Model Selection (Figure 1C). LAP-YIP yeast displaying wild-type LplA or the less-active ^{W37A}LplA mutant were mixed in wt:W37A ratios of 1:100 and 1:10 and labeled for 3 h as described in Lipoylation on the Yeast Cell Surface (Figure 1B). After incubation with fluorophore-conjugated antibodies, 10^7 cells from each mixture were sorted. The top 0.1% and top 1.0% of the PE/AlexaFluor-488 double-positive population for the 1:100 and 1:10 experiments, respectively, were collected. Collected cells were cultured until they reached saturation in SDCAA growth medium (synthetic defined with dextrose and Casamino acids; see the Supporting Information for the recipe) with 50 μg/mL penicillin, 25 μg/mL kanamycin, and 50 μg/mL streptomycin. Plasmid DNA was harvested using the Zymoprep Yeast Plasmid Miniprep kit (Zymo Research), and the recovered LplA genes were amplified using the primers PctAmp-F (5′-CGTTCCAGACTACGCTCTGCAG) and PctAmp-R (5′-CGAGATCTGATAACAACAGTGTAG) and sent for sequencing analysis. Pre- and postsort yeast were repropagated, labeled again as described above, and analyzed by FACS for qualitative comparison. Quantitative analysis of enrichment from pre- to postsort was conducted by analyzing peak intensities on the sequencing chromatogram.

Creating LplA Libraries A and B. The round zero (R0) LplA libraries were cloned into LAP-YIP yeast using gap repair homologous recombination. For library A, the template ^{W37A}LplA gene was mutagenized in polymerase chain reaction (PCR) mixtures containing 2 μM 8-oxo-2′-deoxyguanosine (8-oxo-dGTP), 2 μM 4-dihydro-8*H*-pyrimido[4,5-*c*][1,2]oxazin-7-one (dPTP), dNTPs (200 μM each), and primers PctAmp-F and PctAmp-R (0.2 μM each), and reaction mixtures were thermocycled 10 times. For library B, the template ^{W37A}LplA gene was mutagenized in PCR mixtures containing 200 μM 8-oxo-dGTP, 200 μM dPTP, dNTPs (200 μM each), and primers PctAmp-F and PctAmp-R (0.2 μM each), and reaction mixtures were thermocycled five times. For libraries A and B, mutagenized genes were further amplified via PCRs without mutagenic dNTP analogues using primers PctAmp-F and PctAmp-R. The pCTCON2-Aga2p vector was prepared by digestion with *NheI* and *Bam*HI and gel-purified. The PCR-amplified inserts and digested pCTCON2 vector were mixed in 1:3 ratios, and LAP-YIP yeast cells were transformed by electroporation of the vector and insert as described previously.[23] Homologous recombination of vector and insert occurred inside the yeast, giving the desired product. Serial dilutions of transformed yeast were plated on SDCAA plates (see the Supporting Information for the recipe), and colonies were counted, to determine transformation efficiencies for each library. A total of $\sim 10^9$ cells from the library cultures were pelleted and induced as described in the Supporting Information.

pAz Labeling and Selections on the Yeast Cell Surface (Figure 2). Yeast cells constitutively displaying the LAP peptide and either the induced LplA libraries or individual clones were pelleted and washed twice with PBS-B. Cells were resuspended to a cell density of 2×10^8 cells/mL in PBS-B with 100−200 μM pAz, 5 mM $Mg(OAc)_2$, and 3 mM ATP and incubated on a rotator at 30 °C for 1−12 h (see Figure 2B for library selection conditions). The reactions were stopped by pelleting the cells and washing them with ice-cold PBS-B containing 100 mM EDTA. Cells were washed twice with ice-cold PBS to remove residual BSA, which inhibits the subsequent click reaction. The ligated pAz was detected by performing Cu-catalyzed click chemistry with biotin-alkyne.

The click reagents were prepared: 500 μM THPTA, 100 μM $CuSO_4$, 2.5 mM sodium ascorbate were mixed and incubated at room temperature for 10 min then diluted with PBS to the appropriate volume for the given final concentrations. Biotin-alkyne was then added to a final concentration of 4 μM. The labeled yeast cells were incubated with the click reagents at room temperature on a rotator for 10 min, pelleted, and washed twice with ice-cold PBS-B. The biotin was detected using phycoerythrin-conjugated streptavidin (SA-PE) (Jackson Immunoresearch) in PBS-B at a 1:50 dilution. The LplA surface expression level was detected using mouse monoclonal anti-HA antibody (Roche) in PBS-B at a 1:200 dilution. Incubation with SA-PE and anti-HA occurred simultaneously at 4 °C for 40 min. Cells were pelleted and washed twice with ice-cold PBS-B. Then the yeast cells were incubated with anti-mouse AlexaFluor-488 secondary antibody (Invitrogen) in PBS-B at a 1:100 dilution for 40 min at 4 °C. Cells were pelleted and washed twice with ice-cold PBS-B and then resuspended in PBS-B to a density of $\sim 1 \times 10^7$ cells/mL for FACS.

For the libraries, sorted cells were cultured until saturation in SDCAA growth medium with 50 μg/mL penicillin, 25 μg/mL kanamycin, and 50 μg/mL streptomycin. After the culture had been saturated, $\sim 10^9$ yeast cells were pelleted and induced in SGCAA (synthetic defined with galactose and Casamino acids; see the Supporting Information for the recipe) for the next round of selection.

Analysis of Yeast Pools from Individual Selection Rounds (Figure 2B). Yeast cells harvested from each round of selection were amplified and induced as described above. All pools were treated identically with 100 μM pAz, 5 mM $Mg(OAc)_2$, and 3 mM ATP for 1 h at 30 °C. Rounds 3 and 4 were also labeled under identical conditions for only 30 min at 30 °C. To sequence individual clones, yeast were plated on SDCAA plates, single colonies were amplified in SDCAA medium, and the plasmid was isolated using the Zymoprep Yeast Plasmid Miniprep kit (Zymo Research). To increase the DNA concentration, LplA genes were amplified via PCR from the plasmid using primers PctAmp-F and PctAmp-R and sent for sequencing analysis.

General Mammalian Cell Culture Methods. Human embryonic kidney (HEK) cells were cultured in minimum essential medium (MEM) (Cellgro) supplemented with 10% (v/v) fetal bovine serum (FBS) (PAA Laboratories). All cells were maintained at 37 °C under 5% CO_2. For imaging, cells were plated as a monolayer on glass coverslips. Adherence of HEK cells was promoted by precoating the coverslip with 50 μg/mL fibronectin (Millipore).

Fluorescence Imaging. Cells were imaged in Dulbecco's phosphate-buffered saline (DPBS) in confocal mode. All images shown were recorded using a Zeiss Axiovert 200M inverted microscope with a 40× oil-immersion objective. This instrument is equipped with a Yokogawa spinning disk confocal head, a Quad-band notch dichroic mirror (405/488/568/647), and 405 (diode), 491 (DPSS), 561 (DPSS), and 640 (DPSS) lasers (all 50 mW). Excitation and emission filter settings were as follows: for CFP, 405 nm laser excitation and 445 nm (50 nm) emission; for YFP and AlexaFluor-488, 491 nm laser excitation and 528 nm (38 nm) emission; for AlexaFluor-568, 561 nm laser excitation and 617 nm (73 nm) emission; for AlexaFluor-647, 640 nm laser excitation and 680 nm (30 nm) emission.

Endoplasmic Reticulum (ER) Labeling (Figure 4). HEK cells were transfected at ~70% confluency with expression plasmids for FLAG-^{W37A}LplA-ER (or variant) (600 ng for a 0.95 cm^2 dish) and LAP-neuroligin (600 ng) using Lipofectamine 2000 (Invitrogen). A nuclear cotransfection marker (H2B-YFP) was used (50 ng). Twenty-four hours after transfection, cells were incubated with 25 μM acetoxymethyl-protected pAz (pAz-AM) in serum-free MEM for 4 h at 37 °C. The medium was then replaced three times over 30 min at 37 °C. The cells were rinsed with DPBS once, and the ligated pAz was detected by Cu-catalyzed click with AlexaFluor-alkyne. The click reagents were prepared as described previously.[5] AlexaFluor-647-alkyne was added to a final concentration of 4 μM. The labeled HEK cells were incubated with the click reagents at room temperature for 10 min, washed twice with 1 mg/mL BSA in DPBS (DPBS-B), and then imaged. For quantification of imaging data, cells with a surface signal:background ratio of >2:1 in the AlexaFluor-647 channel were selected for analysis using Slidebook v5.0-defined regions of interest (ROI). The fluorescence intensity background on glass was used to determine the background-corrected mean intensity data for each ROI, which was calculated using Slidebook v5.0 for ~50 cells for each condition.

Trans pAz Ligation on the Mammalian Cell Surface (Figure 5A). One 0.95 cm^2 dish of HEK cells was transfected with FLAG-^{W37A}LplA-neurexin-1β (or variant). Another 0.95 cm^2 dish of HEK cells was transfected with LAP-neuroligin-1 (600 ng) and a nuclear CFP cotransfection marker (H2B-CFP, 50 ng). Transfection was performed at ~70% confluency using Lipofectamine 2000 (Invitrogen). Four hours after transfection, transfection medium was removed and cells were incubated with 2 units/mL DNase in DPBS for 3 min, washed twice with MEM, and placed back in the incubator with complete medium. After being incubated for 6−8 h, cells from each dish were rinsed quickly once with DPBS and then incubated with trypsin-EDTA for 5 min at 37 °C. The two pools of cells were then mixed and coplated on fresh coverslips coated with 50 μg/mL fibronectin (Millipore). After being coplated, cells were incubated in complete medium for 12−24 h and then labeled. For labeling, cells were incubated with 100 μM pAz, 5 mM $Mg(OAc)_2$, and 3 mM ATP in serum-free MEM for 5 min at room temperature. The cells were then rinsed with MEM twice and DPBS once. Cu-catalyzed click chemistry was performed as described previously in Endoplasmic Reticulum (ER) Labeling (Figure 4). The LplA surface expression level was detected on live HEK cells using mouse monoclonal anti-FLAG antibody (Stratagene) in DPBS-B at a 1:300 dilution with incubation at room temperature for 10 min. After being washed, cells were incubated with anti-mouse AlexaFluor-488 secondary antibody (Invitrogen) in DPBS-B at a 1:300 dilution for 10 min at room temperature. Cells were washed twice with DPBS-B and then imaged.

GRASP Comparison (Figure 5B). One 0.95 cm^2 dish of HEK cells was transfected with sfGFP1-10 fused to neurexin-1β (or a variant, 400 ng) and a whole-cell mCherry cotransfection marker (50 ng). Another 0.95 cm^2 dish of HEK cells was transfected with sfGFP11-neuroligin-1 (400 ng) and a nuclear BFP cotransfection marker (nBFP, 50 ng). Transfection was performed at ~70% confluency using Lipofectamine 2000 (Invitrogen). Coplated cultures were prepared as described in Trans pAz Ligation on the Mammalian Cell Surface (Figure 5A). After being coplated, cells were incubated in complete medium for 20 h and then imaged.

Trans pAz and GRASP Image Quantification. Cells with surface labeling in the AlexaFluor-647 channel (for trans pAz labeling) or GFP channel (for GRASP labeling) were selected

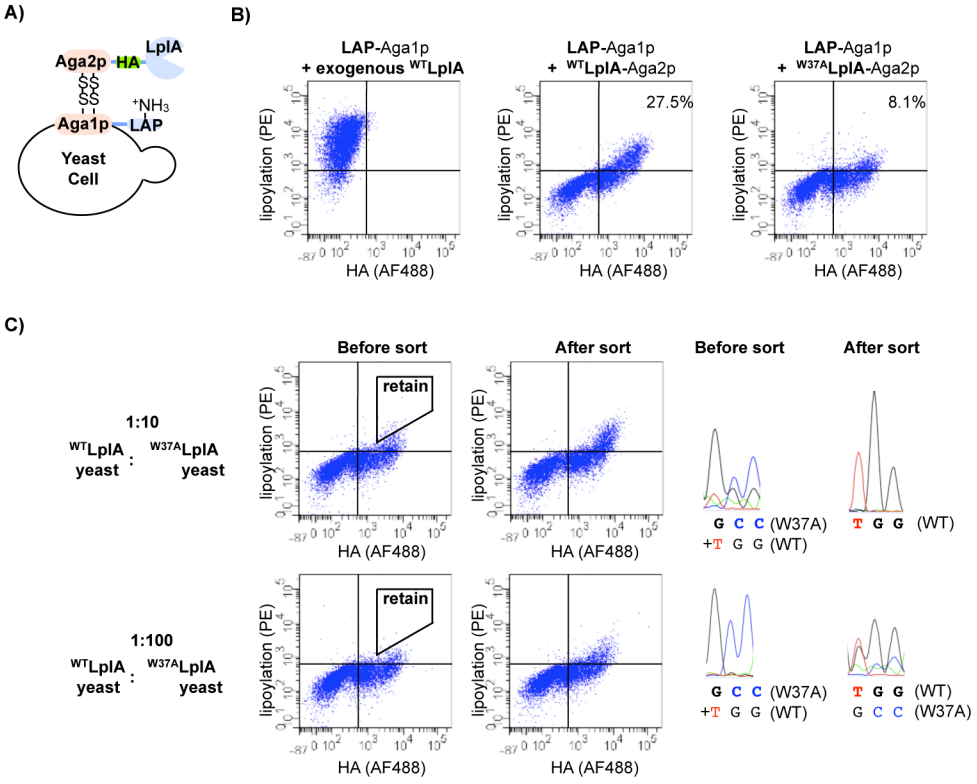

Figure 1. Model selection with LplA and its acceptor peptide codisplayed on the yeast cell surface. (A) Yeast cells constitutively express the LplA acceptor peptide (LAP) as a fusion to the Aga1p surface protein. A subset of these yeast cells transiently express HA-tagged LplA as a fusion to Aga2p. (B) FACS analysis of yeast cells treated with lipoate and ATP to allow *cis* lipoylation of LAP by codisplayed LplA and the ^{W37A}LplA mutant. After incubation with labeling reagents for 3 h, lipoylated LAP is detected with an anti-lipoic acid antibody [phycoerythrin (PE), *y*-axis]. The LplA expression level is quantified using an anti-HA antibody (AF488, *x*-axis). A control using exogenously supplied ^{WT}LplA is shown in the left-most panel. (C) Model selections for enriching ^{WT}LplA-expressing yeast over the less active ^{W37A}LplA-expressing yeast. Yeast cells expressing ^{WT}LplA and ^{W37A}LplA were mixed and then incubated with lipoic acid and ATP for 3 h, stained as in panel B, and FACS sorted using a trapezoidal gate. Sequencing chromatograms of residue 37 of the LplA gene are shown before and after a single round of sorting selection.

for analysis using Slidebook v5.0. For approximately 75 labeled cells under each condition, a point-of-contact surface ROI (signal) and an intracellular ROI (background) were selected for each cell. The fluorescence intensity background on glass was used to determine the corrected mean intensity data for each ROI. The corrected signal:background ratios for each individual cell were calculated, and the average signal:background ratio is reported for each condition.

RESULTS AND DISCUSSION

Selection Platform Based on Codisplay of the Ligase and Peptide on the Yeast Cell Surface. We proposed using a yeast-display system pioneered by Chen and colleagues.[20] In this system, the enzyme and a peptide substrate are codisplayed on the yeast cell surface and enzymatic activity is monitored by modification of the codisplayed substrate (*cis* labeling). This generalizable method was first used to evolve a sortase variant with a 140-fold increase in activity.[20] For our purposes, we prepared yeast constitutively expressing the LAP peptide as a fusion to the Aga1p mating protein. We note that the yeast-surface experiments and library selections were performed with a LAP variant (GFEIDKVWSDLDA, target lysine underlined), while all *in vitro* and mammalian cell-surface experiments were performed with the optimal LAP for those applications (GFEIDKVWYDLDA). We then induce the expression of the LplA enzyme library, which is displayed as a fusion to Aga2p (Figure 1A). After applying labeling reagents to the cells, we can measure the extent of *cis* labeling of the LAP peptide catalyzed by the tethered enzyme. Although the labeling and detection are performed at the cell surface, this strategy will select for LplA variants that retain high activity after being processed through the secretory pathway.

There is the potential for artificially low turnover when using a surface-tethered ligase because of limited access to the surface-expressed peptide. This is particularly true on the yeast cell surface, which is less fluid than the mammalian cell surface.[24] To first demonstrate that *cis* labeling is possible using this platform, yeast displaying ^{WT}LplA and the LAP peptide were incubated with lipoic acid and ATP for 3 h. After antibody staining, the fluorescently labeled yeast pools were analyzed by fluorescence-activated cell sorting (FACS). When yeast cells displaying ^{WT}LplA were analyzed, *cis* lipoylation of LAP was observed, but the signal was not as high as that of identically prepared yeast cells lipoylated using exogenously applied enzyme (Figure 1B). This control is consistent with our previous observations that ^{WT}LplA has decreased activity when expressed on the mammalian cell surface (Figure S1A and supporting methods of the Supporting Information). We also observed a lower-amplitude lipoylation signal when we performed *cis* lipoylation using yeast cells expressing ^{W37A}LplA, although the enzyme expression level was similar (Figure 1B). This result demonstrates that by using the *cis* labeling assay we can distinguish between homogeneous

dx.doi.org/10.1021/bi400268m | *Biochemistry* 2013, 52, 3728−3739

populations of a highly active ligase (^{WT}LplA) and a less active ligase (^{W37A}LplA).

We next wanted to demonstrate that this selection strategy can enrich the population of highly active ligases from a heterogeneous sample. To do this, we performed one round of model selection on mixtures of ^{WT}LplA and ^{W37A}LplA yeast. For the model selections, yeast cells were mixed in 1:10 and 1:100 ^{WT}LplA:^{W37A}LplA yeast ratios and then labeled with lipoic acid. After antibody staining, cells that exhibited a high ratio of labeling to enzyme expression were sorted via FACS (Figure 1C). Before the cells had been sorted, the population of highly labeled yeast decreased with an increasing dilution of ^{WT}LplA; after the cells had been sorted, the population of highly labeled yeast was enriched. In one round of model selection, we observed 50-fold enrichment of ^{WT}LplA over ^{W37A}LplA (Figure 1C, chromatograms). These results demonstrate that detection of LAP *cis* labeling is an effective readout of overall enzyme activity and that the selection strategy enriches the population of ligases with high ligation activity.

Directed Evolution of a Picolyl Azide (pAz) Ligase. After validating the evolution platform using a model selection for lipoic acid, we wanted to select for an LplA variant with improved activity for a useful small molecule probe. Direct fluorophore ligation using PRIME is ideal for intracellular applications, as there is only one probe washout step. However, we proposed the use of a two-step labeling scheme in which LplA is used to ligate a functional group handle, which can then be chemoselectively derivatized with a variety of probes. A two-step strategy is advantageous because one enzyme evolution step can allow protein labeling with virtually any fluorophore or probe.

To accurately reflect the relative activity of the first enzymatic step in the selections, the second derivatization step needs to be both fast and high-yielding. For yeast cell-surface labeling, it also needs to be cell-compatible. Recent work introduced a method for cell-compatible click chemistry using a copper-chelating picolyl azide (pAz).[5] The high specificity of the enzymatic pAz ligation, combined with the fast kinetics and minimal cytotoxicity of the modified click step, makes this an ideal selection strategy for yeast-display evolution of LplA. The general pAz selection strategy is shown in Figure 2A. In the first step, the yeast cells are incubated with pAz and ATP, allowing for enzymatic ligation of the pAz probe to LAP on the cell surface. Then, to maximize the fluorescent labeling signal, cell-compatible copper click is performed with a biotin-alkyne followed by detection with phycoerythrin-conjugated streptavidin (SA-PE). This protocol produces an effective fluorescent readout of enzymatic pAz ligation activity.

Before performing any selections, we first tested pAz labeling on the yeast cell surface using the best rationally designed azide ligases. This would provide a benchmark for the library selection. We tested the pAz *cis* ligation activity using ^{W37V}LplA and ^{W37A}LplA, the two most active pAz ligases *in vitro*.[5] While pAz labeling of the LAP yeast using exogenous ^{W37V}LplA produced a very strong signal in just 1 h, no *cis* labeling was observed with either ^{W37V}LplA or ^{W37A}LplA, even after incubation of the probe for 12 h (Figure 2A). In fact, it required incubation of the probe for 20 h before any *cis* labeling with ^{W37A}LplA was observed (Figure 2A). This result further emphasizes the decreased activity of LplA when it is expressed on the cell surface.

The next step was to create LplA enzyme libraries for the pAz-based activity selections. Although ^{W37V}LplA is the best pAz ligase *in vitro*, the libraries were made using ^{W37A}LplA as the template. We chose ^{W37A}LplA because this enzyme has expression superior to that of ^{W37V}LplA on the yeast cell surface, has been shown to ligate the pAz probe *in vitro*,[5] and produced some *cis* labeling signal at long probe incubation times (Figure 2A). Error-prone PCR was used to generate libraries of LplA mutants (see Experimental Procedures for details). Because it was not initially clear whether a high mutation rate would be beneficial or deleterious to the activity of LplA, two libraries were produced with varying mutation rates. The first library, library A, was made using a low mutation rate, with one to two nonsilent mutations per gene (8.0×10^7 transformants). Library B was made using a moderate mutation rate of one to six nonsilent mutations per gene (2.5×10^7 transformants).

Each library was independently subjected to four rounds of selection for pAz ligation; yeast pools were amplified between rounds, but no further library diversification was performed. Evolutionary pressure for improved catalytic activity was introduced by decreasing the labeling times (from 12 to 1 h) and by collecting a smaller fraction of cells in each successive round. For rounds 3 and 4, we applied additional evolutionary pressure for improved pAz substrate recognition by reducing the concentration of the pAz probe used for the labeling (from 200 to 100 μM). After completing four rounds of selection, we assayed the yeast from each round under identical conditions to validate the selection strategy (Figure 2B). While enzyme expression levels (x-axes) remained relatively constant through each round of selection, we observed a steady increase in pAz labeling intensities (y-axes), with the maximal labeling signal observed by round 4. From these FACS data, we concluded that the selection strategy successfully enriched library members with improved pAz ligation activity.

To monitor library diversity and identify trends in conserved mutations, sequencing analysis was performed on clones isolated from each round for each of the libraries (Figure S2 of the Supporting Information). For library A, the size of the original library (8.0×10^7 members) was reduced through four rounds of selection to just two consensus clones (A4.6 and ALR [W37A/F147L/H267R]), while the size of library B was reduced from 2.5×10^7 members to three consensus clones (B4.2, B4.3, and B4.8). We noted that the majority of highly conserved mutations were located either in the C-terminal domain of LplA (after residue 256) or in areas far from the small molecule binding pocket (*vide infra*).

Evaluation of Evolved Ligase Mutants on the Yeast and Mammalian Cell Surface. We first tested the activity and specificity of the individual consensus clones on the yeast cell surface. The relative activities of the five consensus clones were compared by performing pAz *cis* ligation onto the LAP peptide (Figure S3 of the Supporting Information). To assess the specificity of pAz labeling, the ligases were expressed on yeast cells constitutively expressing the acceptor peptide for biotin ligase (AP), which should not be recognized by LplA or its variants. We then performed a *cis* labeling experiment using the nonsubstrate AP yeast, and while most of the consensus clones were highly specific, some nonspecific labeling of AP was observed with B4.3 (Figure S3 of the Supporting Information).

The next goal was to demonstrate that the evolved activity is not context-dependent, that strong pAz labeling can be achieved even when the enzymes are taken out of the context of the yeast cell surface. To that end, we developed an assay to test *cis* pAz labeling on the surface of mammalian cells. The

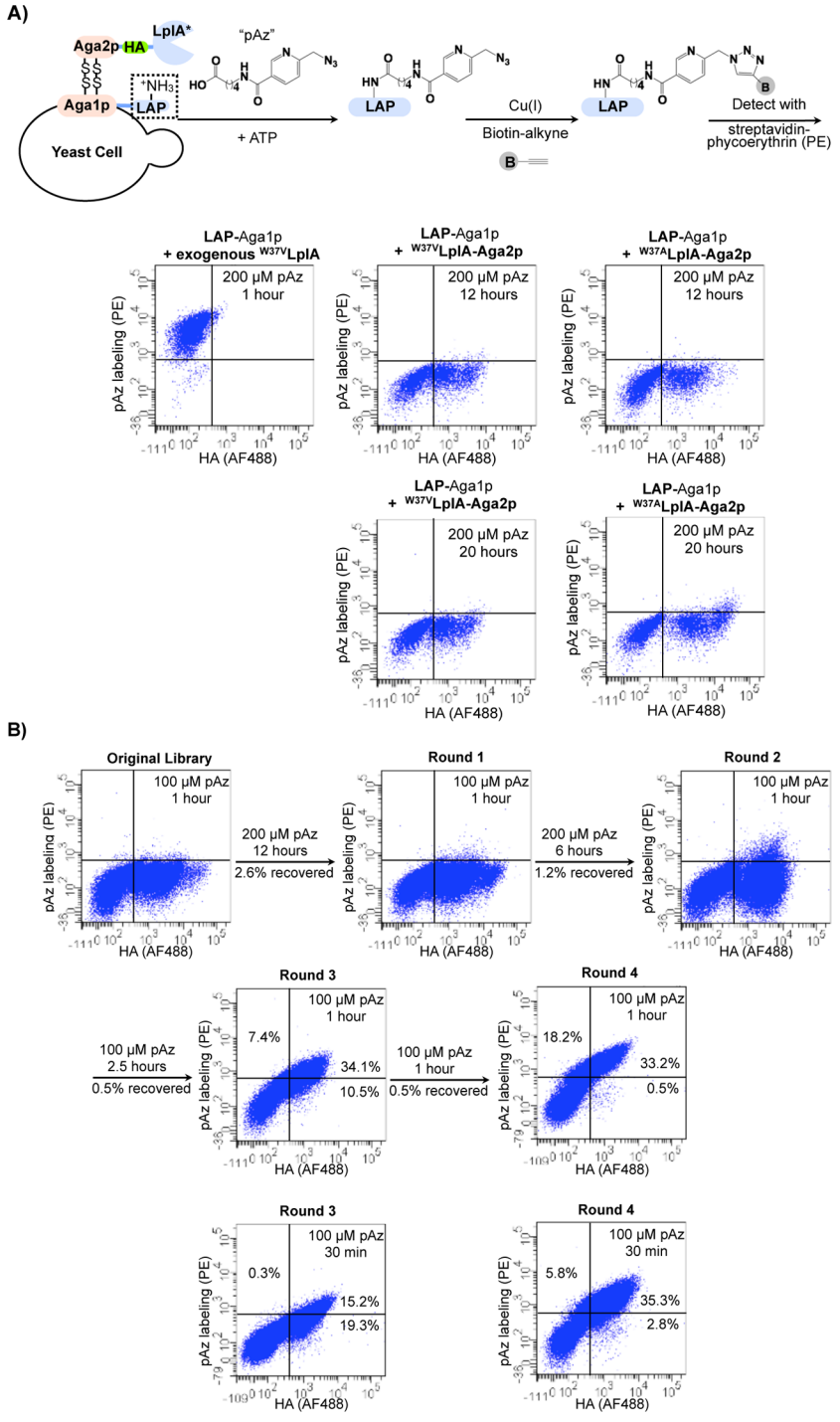

Figure 2. Selection for LplA mutants with picolyl azide ligation activity on the yeast surface. (A) Selection scheme. The LAP peptide and an LplA library (LplA*, error-prone PCR of the ^{W37A}LplA template) are codisplayed on the yeast surface as in Figure 1A. Each yeast cell displays a single LplA mutant. The yeast cells are incubated with the picolyl azide probe (pAz) and ATP. LAP-conjugated pAz is detected by click chemistry with biotin-alkyne, followed by staining with streptavidin-phycoerythrin (PE, *y*-axis). The left-most FACS plot shows pAz labeling using exogenously applied ^{W37V}LplA in a 1 h reaction. The remaining plots show *cis* pAz4 labeling of LAP by codisplayed ^{W37A}LplA or ^{W37V}LplA in 12 and 20 h reactions. The LplA expression level is quantified using an anti-HA antibody (AF488, *x*-axis). (B) FACS analysis of reamplified yeast pools after four rounds of selection on LplA library A. Selection conditions used for each round are listed above the arrows. Percentages of cells recovered in each round are given beneath the arrows. The first five FACS plots show labeling of the original library and reamplified yeast pools using reaction times of 1 h. Round 3 and round 4 pools were also analyzed using reaction times of 30 min (last two plots).

ligases were expressed as fusions to neurexin-1β (NRX). Neurexin-1β was chosen because this neuronal adhesion protein is expressed well on the mammalian cell surface, and we previously demonstrated that ^{WT}LplA can catalyze the ligation of lipoic acid in *cis* when fused to this protein (Figure S1A of the Supporting Information). For easy quantification of the substrate expression level, a fusion of LAP to CFP was co-expressed with the ligase on the HEK cell surface. The cells were incubated with ATP and pAz, which was followed with click chemistry using an AlexaFluor-647-alkyne (Figure S4A of

dx.doi.org/10.1021/bi400268m | *Biochemistry* 2013, 52, 3728−3739

the Supporting Information). In this assay, we observed labeling of the LAP peptide using all of the mutants, demonstrating that labeling with the evolved ligases is not dependent on a yeast-display context. To better assess activity trends, we quantified the magnitude of the labeling signal and compared it to both enzyme and substrate expression levels (Figure S4C of the Supporting Information). The highest ratios were observed with ^{ALR}LplA. While consistent with the yeast cell-surface activity trends, the *cis* labeling signal observed when using the evolved ligases on the mammalian cell surface was still 3−8-fold weaker than the exogenous labeling signal.

We sought to further improve the pAz labeling activity of the evolved ligases by incorporating additional beneficial mutations. Through our extensive work engineering LplA, we have discovered that Thr57 of LplA is a critical position in the enzyme and when Thr57 is mutated to isoleucine (T57I) LplA cell-surface lipoylation activity is improved (Figure S1B of the Supporting Information). We hypothesized that this mutation might also improve the pAz ligation activity of the evolved ligases. To test this, we added the T57I mutation to the most active evolved ligase, ^{ALR}LplA (W37A/F147L/H267R), to create ^{AILR}LplA (W37A/T57I/F147L/H267R). When this new mutant was included in the *cis* mammalian cell assay, we found the ^{AILR}LplA was more active than ^{ALR}LplA and produced a *cis* pAz labeling signal that was equivalent to the exogenous enzyme under all conditions tested (Figure S4 of the Supporting Information). To ensure that the labeling could be generalized, we tested *cis* labeling of LAP fused to neuroligin-1 (LAP-NLG) and observed a similar increase in activity (Figure S4B of the Supporting Information). When the labeling signal was quantified and compared to both the enzyme expression level and the substrate expression level, ^{AILR}LplA outperformed all of the evolved ligases in the *cis* ligation assay (Figure S4C of the Supporting Information). With this result, we determined that ^{AILR}LplA is the best pAz ligase for mammalian cell-surface applications.

Characterization of the Evolved pAz Ligase. After demonstrating that ^{AILR}LplA produces the strongest pAz labeling signal on the mammalian cell surface, we wanted to characterize its activity *in vitro*. Figure 3A shows HPLC traces from 10 min *in vitro* LAP (GFEIDKVWYDLDA) labeling reactions using ^{AILR}LplA and other ligases under identical labeling conditions. The identity of the LAP−pAz conjugate was confirmed by mass spectrometry (Figure S5A of the Supporting Information). A control experiment in which ATP was omitted demonstrated that pAz ligation using ^{AILR}LplA is ATP-dependent. Similar HPLC activity assays were performed at lower probe concentrations (50 μM pAz). Both ^{AILR}LplA and ^{ALR}LplA produced more LAP−pAz product in these assays than the best rationally designed ligase, ^{W37V}LplA (Figure 3B). Encouraged by the *in vitro* results, we measured the kinetics of ligation of pAz onto LAP. For ^{AILR}LplA, we determined the k_{cat} to be 0.34 s^{-1}, while for ^{ALR}LplA, we calculated a k_{cat} of 0.39 s^{-1} (Figure S5B of the Supporting Information); these values can be compared to those calculated for ^{W37A}LplA and ^{W37V}LplA (k_{cat} values of 0.08 and 0.19 s^{-1}, respectively). The k_{cat} values for pAz ligation using the evolved and optimized ligases are 2−4-fold higher than those for the best rationally designed ligases and 15−20-fold higher than those for *in vitro* coumarin ligation.[1] This result confirms that the evolutionary pressure applied during the selections was successful in enriching ligases with improved catalytic activities.

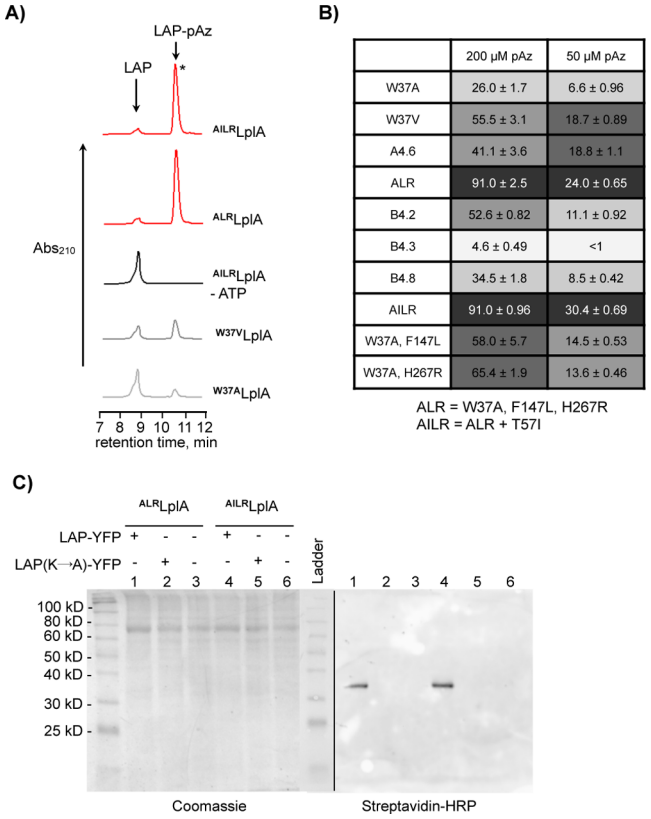

	200 μM pAz	50 μM pAz
W37A	26.0 ± 1.7	6.6 ± 0.96
W37V	55.5 ± 3.1	18.7 ± 0.89
A4.6	41.1 ± 3.6	18.8 ± 1.1
ALR	91.0 ± 2.5	24.0 ± 0.65
B4.2	52.6 ± 0.82	11.1 ± 0.92
B4.3	4.6 ± 0.49	<1
B4.8	34.5 ± 1.8	8.5 ± 0.42
AILR	91.0 ± 0.96	30.4 ± 0.69
W37A, F147L	58.0 ± 5.7	14.5 ± 0.53
W37A, H267R	65.4 ± 1.9	13.6 ± 0.46

ALR = W37A, F147L, H267R
AILR = ALR + T57I

Figure 3. Characterization of evolved (^{ALR}LplA) and optimized (^{AILR}LplA) picolyl azide ligases. (A) HPLC traces showing conversion of the LAP peptide to the picolyl azide conjugate (LAP−pAz), catalyzed by ^{W37A}LplA, ^{W37V}LplA, or the evolved mutants ^{ALR}LplA and ^{AILR}LplA. A negative control which omitted ATP is colored black. The starred product peak was collected and analyzed by mass spectrometry in Figure S5A of the Supporting Information. (B) Table showing percent conversions of LAP to the LAP−pAz conjugate catalyzed by various LplA mutants. The first column corresponds to the reaction conditions used in panel A: 200 μM pAz and 2 μM ligase for 10 min. In the second column, the pAz concentration is reduced to 50 μM. The last two rows show contributions of individual mutations in ^{ALR}LplA to pAz ligation activity. Measurements were performed in triplicate. Errors are one standard deviation. (C) Sequence specificity of evolved ^{ALR}LplA and ^{AILR}LplA mutants for LAP labeling in mammalian cell lysate. Lanes 1 and 4 show ligation of pAz to LAP-YFP (32 kDa) catalyzed by ^{ALR}LplA and ^{AILR}LplA, respectively. pAz was detected by click cycloaddition with biotin-alkyne followed by streptavidin−HRP blotting. Negative controls are shown with an alanine mutation in LAP (lanes 2 and 5) and untransfected lysate (lanes 3 and 6).

We note that the trends for *in vitro* pAz ligation activity correlate well with trends we observe on both the mammalian and yeast cell surface. All of the evolved ligases, except for B4.3, have improved *in vitro* activity compared to that of ^{W37A}LplA, the library starting point (Figure 3B). However, only the ALR and AILR mutants demonstrate improved *in vitro* pAz labeling compared to that of the best rationally designed ligase, ^{W37V}LplA. We found that, for pAz ligation, the effects of the F147L and H267R mutations in combination are largely additive. We also observed that ^{AILR}LplA did not show improvement over ^{ALR}LplA at high pAz probe concentrations, and only minimal improvement at the lower pAz probe concentration (Figure 3B). This result contrasts with the mammalian cell-surface data, which showed that the addition of

dx.doi.org/10.1021/bi400268m | *Biochemistry* 2013, 52, 3728−3739

T57I drastically improved pAz labeling activity. Given these results, we hypothesize that the T57I mutation may stabilize the enzyme when expressed on the cell surface and is neither advantageous nor deleterious when working with purified enzymes. This hypothesis is supported by the result that there is no change in *in vitro* lipoylation k_{cat} when the T57I mutation is incorporated into ^{WT}LplA (Figure S5C of the Supporting Information).

We next investigated how the two evolved mutations (F147L and H267R) might be contributing to overall activity improvements of the enzyme. We first hypothesized that the F147L mutation was involved in accommodating the bound azide structure or contributing to pAz catalysis in a probe-specific manner because of its location above the lipoyl-AMP binding pocket in LplA (Figure S6 of the Supporting Information). This hypothesis is supported by the observation that when the F147L mutation is introduced into wild-type LplA, it does not improve the k_{cat} for lipoylation (Figure S5C of the Supporting Information). However, two results indicate that this hypothesis might be incorrect. First, when we used a probe-AMP docking protocol[4] to dock the energy-minimized pAz-AMP structure into the lipoyl-AMP binding pocket of LplA,[25] we found that the F147L mutation is not proximal to the azide moiety, which places in doubt the direct involvement of the F147L mutation in pAz binding or recognition. Second, in contrast to the result obtained when the F147L mutation was added to ^{WT}LplA, we observed significantly improved lipoylation activity when the F147L mutation was combined with the W37A mutation (Figure S5D of the Supporting Information). This result indicates that the F147L mutation may be a potentiating mutation that improves enzyme activity only when Trp37 is also mutated.

Unlike the F147L mutation, the H267R mutation seems to generally increase enzyme activity in a manner independent of the small molecule probe being used (Figure S5C,D of the Supporting Information). His267 is located at the interface between the N- and C-terminal domains of the apo LplA structure[26] (Figure S6 of the Supporting Information). LplA undergoes a global conformational change after formation of the lipoyl-AMP and before transfer to the protein substrate.[25] Upon formation of the adenylate ester, the C-terminal domain of LplA flips approximately 180°, adopting a stretched conformation and exposing the site of protein substrate binding (Figure S6 of the Supporting Information). We propose that the mutation of His267 to a bulky arginine residue is helping to promote this global conformational change by pressing the C-terminal domain away from the N-terminal domain and preordering the open conformation of the enzyme[25] (movie of the Supporting Information). Consistent with this hypothesis, when the H267R mutation is introduced into wild-type LplA, we notice a 2-fold improvement in the k_{cat} of the wild-type lipoylation reaction (Figure S5C of the Supporting Information). The other individual mutations of ^{AILR}LplA did not produce this increase in lipoylation activity when introduced into the wild-type ligase, which suggests that the contributions of these mutations to improved pAz ligation activity may be the result of probe-specific effects or require coincidence of the W37A mutation. It is also possible that the rate enhancement effects are only evident in the context of cell-surface expression and stability and are thus less apparent when performing *in vitro* reactions.

Before testing the optimized clone in mammalian cells, we confirmed the sequence specificity of ^{AILR}LplA on cell lysate. The lysate from HEK cells expressing LAP fused to yellow fluorescent protein (LAP-YFP) was prepared, and we performed pAz labeling using either ^{AILR}LplA or ^{ALR}LplA (Figure 3C). While lanes 1 and 4 demonstrate specific ligation of pAz to LAP-YFP, control lanes using untransfected lysate or lysate from cells expressing a LAP mutant with the target lysine mutated to an alanine do not show labeling. These results demonstrate that the evolved pAz ligases retain the exquisite sequence specificity of the original LplA.

Yeast-display evolution was selected because we predicted that increased activity on the yeast cell surface would translate to increased activity in the ER. We therefore wanted to test the ability of the optimized pAz ligase (^{AILR}LplA) to label proteins when it is expressed in the ER. To increase intracellular probe concentration and improve labeling signal, we used a cell-permeable form of the pAz probe with an acetoxymethyl protecting group (pAz-AM). In HEK cells, the ligase was targeted to the ER using a KDEL motif and co-expressed with LAP-neuroligin-1, which can be labeled by the ER enzyme as it is transported through the secretory pathway (Figure 4A). When using ER-targeted ^{AILR}LplA, LAP-neuroligin-1 was strongly labeled (Figure 4B). This is the first demonstration of PRIME labeling using an ER-targeted ligase. We do note that pAz labeling using exogenously applied enzyme is still 3−4-fold stronger than when using ^{AILR}LplA-ER, indicating that enzyme activity in the ER can still be further improved (Figure 4C).

Application to Labeling Protein−Protein Interactions. Finally, we wanted to apply ^{AILR}LplA to the labeling of intercellular contacts and explore the potential for using the evolved ligase to extend ID-PRIME and allow for the labeling of intercellular protein−protein interactions. To do this, we proposed investigating the interactions of neurexin and neuroligin between living mammalian cells. Neurexin is a presynaptic adhesion protein, and neuroligin is its postsynaptic interacting partner. Through various *in vitro* and *in vivo* experiments, neurexin and neuroligin have been implicated in synapse initiation and maturation.[27−30] However, investigation of the biological relevance of these results has so far been limited by the live cell imaging techniques available. We envision that the evolved pAz PRIME ligase will be a useful tool in exploring protein−protein interactions between cells and at subdiffraction-limited sites such as the synapse.

While the ultimate goal is to label neurexin and neuroligin interactions at a synapse, where this interaction is biologically relevant, intercellular labeling in HEK cells serves as an important proof of principle. First, we developed a *trans* pAz labeling assay to test the ability of ^{AILR}LplA to label intercellular contacts between HEK cells. In this assay, we transfect one pool of HEK cells with ^{AILR}LplA-neurexin-1β and a separate pool of HEK cells with LAP-neruoligin-1. After transfection, the two populations are lifted, mixed, and coplated on the same coverslip. If the ligase can successfully label intercellular protein−protein contacts, then contact points between the two populations of HEK cells should result in labeling of the LAP-neuroligin by the ^{AILR}LplA-neurexin (Figure 5A, scheme).

Figure 5A shows that we are able to label the intercellular contact of these two proteins with just a 5 min pAz labeling protocol in HEK cells. Controls in which the experiment was performed identically but using either ^{W37A}LplA or the alanine mutant of LAP demonstrate the specificity of the intercellular labeling. Interestingly, when *trans* pAz labeling is performed using ^{AILR}LplA, the labeling signal observed after the 5 min labeling protocol is better than that observed when using

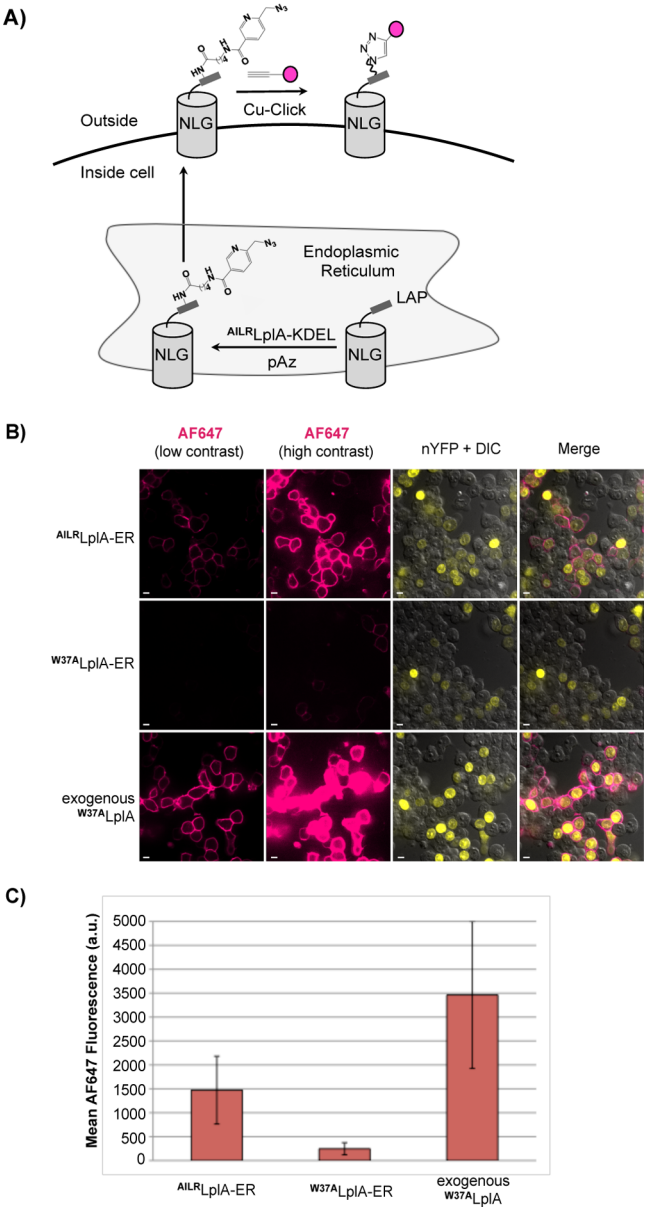

Figure 4. Activity of ^{AILR}LplA in the ER of live cells. (A) Scheme. LAP-neuroligin-1 (NLG) (N-terminal LAP facing the ER lumen) is labeled using a ligase retained in the ER via a KDEL tag. pAz-labeled LAP-NLG that reaches the cell surface can be detected by click chemistry with AF647-alkyne. (B) HEK cells co-expressing ER-targeted ligase, LAP-NLG, and a nuclear YFP (nYFP) transfection marker were treated with pAz-AM for 4 h. Click chemistry was performed at the cell surface. Panels show imaging results for ^{AILR}LplA (top) and ^{W37A}LplA (middle). For comparison, the bottom row shows the signal obtained with exogenous ^{W37A}LplA. Confocal images; 10 μm scale bars. (C) Bar graph showing the quantification of the labeling signal (~50 cells) for each condition. Errors are one standard deviation.

exogenously applied enzyme. After this promising result, we next determined whether the labeling signal observed in the *trans* assay is dependent on the interaction between neurexin and neuroligin. To test this, we performed the *trans* labeling experiment using a fusion of ^{AILR}LplA to an interaction-deficient mutant of neurexin-1β (^{D137A}NRX) (Figure 5A). Although a few intercellular contacts were labeled using the interaction-deficient version of neurexin, the labeling signal never exceeded 15% of what we observed in the presence of protein−protein interaction. This control demonstrates that labeling is largely interaction-dependent. We have since extended this *trans* pAz labeling method to the imaging of synaptic partners in live neurons.[31]

Finally, we wanted to compare our method to the GRASP methodology (GFP reconstitution across synaptic partners), another method that can image protein−protein interactions in live cells. This method uses a split superfolder GFP (sfGFP) to image protein−protein contacts across cells or synapses;[32,33] the large portion of sfGFP is fused to one interacting partner, and the remaining smaller portion of sfGFP is fused to the other interacting partner. When expressed separately, the two proteins are nonfluorescent. Upon colocalization of the protein partners, the sfGFP is reconstituted, trapping the interacting proteins in a complex, with the sfGFP becoming fluorescent after chromophore maturation (Figure 5B, scheme). This method has recently been used to image protein−protein contacts across synapses in tissue culture and even in transgenic mice.[32]

We first tried the *trans* experiment using the exact GRASP constructs described in the work of Kim and colleagues, where the larger piece of sfGFP is fused to CD4 and the smaller piece of sfGFP is fused to neuroligin-1.[33] These constructs were designed as a pair that would report on synapse formation as determined by spatial proximity. Unfortunately, we were not able to observe GFP complementation in a *trans* assay in HEK cells, despite observing GFP complementation when the two pieces were expressed in the same cell (data not shown). We hypothesized that when these constructs are expressed in neurons, scaffolding proteins and endogenous protein assemblies force the intercellular interaction of CD4 and neuroligin, which in turn promotes sfGFP complementation. In support of this hypothesis, when the sfGFP pieces were fused to neurexin-1β and neuroligin-1, which we have already demonstrated interact well across HEK cells, we observed GFP complementation in the *trans* assay (Figure 5B). Moreover, when we used an interaction-deficient form of neurexin-1β, we observed a significant decrease in the number of GFP complementation events and a decrease in the GFP fluorescence intensity of those events. These two results, taken together, suggest that the GRASP method may indeed be interaction-dependent in some contexts.

To directly compare the GRASP method and our pAz labeling method, the labeling signal to background ratio was determined for each protocol (additional fields of view for both experiments can be found in Figures S7 and S8 of the Supporting Information). We found that the *trans* pAz ligation method gives a signal to background ratio of 26, while the GRASP method produces a signal to background ratio of 11. This indicates that the *trans* pAz labeling technique is more sensitive than GRASP, producing a stronger signal for a given protein−protein interaction.

CONCLUSIONS

Using yeast-display evolution of *E. coli* lipoic acid ligase, we have engineered a PRIME ligase (^{AILR}LplA) with improved picolyl azide labeling properties. We have demonstrated the improved pAz ligation activity of this ligase *in vitro* and also report the demonstration of PRIME labeling using enzyme expressed on the surface of living cells and in the endoplasmic reticulum. While there have been other recent examples using yeast display to produce improved enzyme catalysis,[20,21,34] to the best of our knowledge this is the first example of the

dx.doi.org/10.1021/bi400268m | *Biochemistry* 2013, 52, 3728−3739

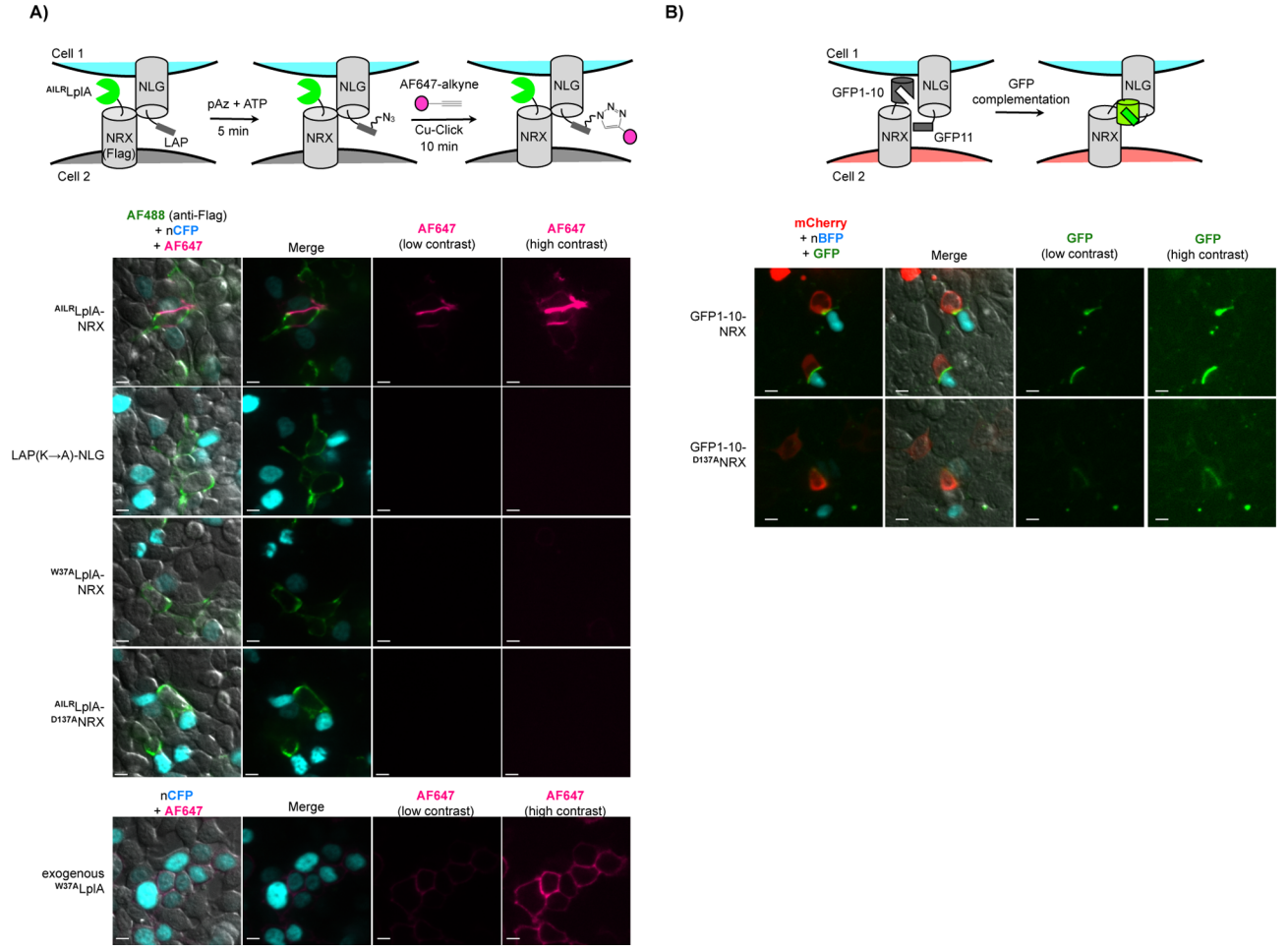

Figure 5. Labeling of trans-cellular neurexin (NRX) and neuroligin (NLG) interactions using the evolved picolyl azide ligase. (A) The top panel shows a scheme for *trans* labeling between ^{AILR}LplA-NRX and LAP-NLG expressed on contacting cells. The bottom panels show images from HEK cells expressing ^{AILR}LplA-NRX, coplated with HEK cells expressing LAP-NLG and a nuclear CFP (nCFP) marker (row 1). ^{AILR}LplA-NRX expression was detected by anti-Flag staining (AF488). AF647, used to derivatize pAz-labeled LAP, is shown at both high and low contrast. Negative controls are shown with an alanine mutation in LAP (row 2), ^{W37A}LplA in place of ^{AILR}LplA (row 3), and a mutation in NRX (D137A) that abolishes its interaction with NLG (row 4). For comparison, the signal obtained from labeling LAP-NLG with exogenous ^{W37A}LplA is shown (row 5). Additional fields of view from this same experiment are shown in Figure S7 of the Supporting Information. Confocal images; 10 μm scale bars. (B) Comparison to the GRASP method for detection of NRX-NLG *trans* interactions. The top panel shows a scheme for *trans* labeling between sfGFP1−10 and sfGFP11 fragments that were fused to the same sites as LplA and LAP, respectively, on NRX and NLG. The bottom panels show images from HEK cells expressing sfGFP1−10-NRX (mCherry cotransfection marker), coplated with HEK cells expressing sfGFP11-NLG (nBFP cotransfection marker) (row 1). GFP is shown at both high and low contrast. A control with the D137A mutation in NRX is included (row 2). Additional fields of view from this same experiment are shown in Figure S8 of the Supporting Information. Confocal images; 10 μm scale bars.

evolution of activity for an application where there was no observable activity using the original enzyme.

The expansion of the PRIME labeling methodologies to the ER designates PRIME as one of the most versatile labeling methods currently available. While other protein-based methods such as SNAP/CLIP[35] and HaloTag[36] can be applied to oxidizing compartments of the cell, the large size of these tags can interfere with target protein function. With the developments described in this paper, the PRIME method now uniquely combines a peptide tag, high labeling specificity, and the ability to label target proteins in both reducing and oxidizing compartments of the cell. Moreover, the variety of fluorophores and probes that can be incorporated using PRIME makes it an attractive method for a wide range of biological applications.

We have further demonstrated the application of this evolved ligase to the labeling of intercellular protein−protein interactions. We were able to use ID-PRIME to label the interaction of neurexin-1β and neuroligin-1 on HEK cells in just 5 min. Compared to the GRASP method for labeling synaptic partners, our method gives a better signal and produces a label that is nontrapping. The application of the PRIME method to imaging synaptic partners in live neurons[31] emphasizes the power and versatility of our evolved ligase. Using our method, we envision that more advanced experiments can be attempted, such as time-lapse imaging following interaction detection to monitor subsequent trafficking of a labeled interacting partner.

■ ASSOCIATED CONTENT

Supporting Information

Figures S1−S8, supporting methods (general yeast methods, methods for LAP-Aga1p yeast preparation, protein purification, *in vitro* assays, and Western blotting of mammalian cell lysate), descriptions of genetic constructs used, and a movie. This

dx.doi.org/10.1021/bi400268m | *Biochemistry* 2013, 52, 3728−3739

material is available free of charge via the Internet at http://pubs.acs.org.

AUTHOR INFORMATION

Corresponding Author

*E-mail: whitek@alum.mit.edu. Phone: (415) 476-1272.

Present Addresses

[†]Department of Cell and Tissue Biology, University of California San Francisco, 513 Parnassus Ave., HSW618, San Francisco, CA 94143.

[‡]University of South Florida Morsani College of Medicine, 12901 Bruce B. Downs Blvd., MDC 2, Tampa, FL 33647.

Notes

The authors declare no competing financial interest.

ACKNOWLEDGMENTS

We thank Chayasith Uttamapinant [Massachusetts Institute of Technology (MIT)] for generously providing the picolyl azide and picolyl azide-AM probes. We thank Irwin Chen [formerly of Harvard University (Cambridge, MA), currently of Amgen] for providing the initial yeast-display plasmids and Sujiet Puthenveetil (formerly of MIT, currently of Pfizer) for supplying the LAP-expressing yeast and providing methodological help in the initial stages of the project. We also acknowledge the helpful comments of Daniel Liu (MIT) during data analysis.

REFERENCES

(1) Uttamapinant, C., White, K. A., Baruah, H., Thompson, S., Fernandez-Suarez, M., Puthenveetil, S., and Ting, A. Y. (2010) A fluorophore ligase for site-specific protein labeling inside living cells. *Proc. Natl. Acad. Sci. U.S.A. 107*, 10914−10919.

(2) Yao, J. Z., Uttamapinant, C., Poloukhtine, A., Baskin, J. M., Codelli, J. A., Sletten, E. M., Bertozzi, C. R., Popik, V. V., and Ting, A. Y. (2012) Fluorophore targeting to cellular proteins via enzyme-mediated azide ligation and strain-promoted cycloaddition. *J. Am. Chem. Soc. 134*, 3720−3728.

(3) Liu, D. S., Tangpeerachaikul, A., Selvaraj, R., Taylor, M. T., Fox, J. M., and Ting, A. Y. (2012) Diels-Alder cycloaddition for fluorophore targeting to specific proteins inside living cells. *J. Am. Chem. Soc. 134*, 792−795.

(4) Cohen, J. D., Thompson, S., and Ting, A. Y. (2011) Structure-guided engineering of a Pacific Blue fluorophore ligase for specific protein imaging in living cells. *Biochemistry 50*, 8221−8225.

(5) Uttamapinant, C., Tangpeerachaikul, A., Grecian, S., Clarke, S., Singh, U., Slade, P., Gee, K. R., and Ting, A. Y. (2012) Fast, Cell-Compatible Click Chemistry with Copper-Chelating Azides for Biomolecular Labeling. *Angew. Chem., Int. Ed. 51*, 5852−5856.

(6) Slavoff, S. A., Liu, D. S., Cohen, J. D., and Ting, A. Y. (2011) Imaging protein-protein interactions inside living cells via interaction-dependent fluorophore ligation. *J. Am. Chem. Soc. 133*, 19769−19776.

(7) Green, D. E., Morris, T. W., Green, J., Cronan, J. E., Jr., and Guest, J. R. (1995) Purification and properties of the lipoate protein ligase of *Escherichia coli*. *Biochem. J. 309* (Part3), 853−862.

(8) Turner, N. J. (2009) Directed evolution drives the next generation of biocatalysts. *Nat. Chem. Biol. 5*, 567−573.

(9) Goldsmith, M., and Tawfik, D. S. (2012) Directed enzyme evolution: Beyond the low-hanging fruit. *Curr. Opin. Struct. Biol. 4*, 406−412.

(10) Turner, N. J. (2003) Directed evolution of enzymes for applied biocatalysis. *Trends Biotechnol. 21*, 474−478.

(11) Zhang, K., Li, H., Cho, K. M., and Liao, J. C. (2010) Expanding metabolism for total biosynthesis of the nonnatural amino acid L-homoalanine. *Proc. Natl. Acad. Sci. U.S.A. 107*, 6234−6239.

(12) Atsumi, S., and Liao, J. C. (2008) Directed evolution of *Methanococcus jannaschii* citramalate synthase for biosynthesis of 1-propanol and 1-butanol by *Escherichia coli*. *Appl. Environ. Microbiol. 74*, 7802−7808.

(13) Blagodatski, A., and Katanaev, V. L. (2010) Technologies of directed protein evolution in vivo. *Cell. Mol. Life Sci. 68*, 1207−1214.

(14) Janda, K. D., Lo, L. C., Lo, C. H., Sim, M. M., Wang, R., Wong, C. H., and Lerner, R. A. (1997) Chemical selection for catalysis in combinatorial antibody libraries. *Science 275*, 945−948.

(15) Seelig, B., and Szostak, J. W. (2007) Selection and evolution of enzymes from a partially randomized non-catalytic scaffold. *Nature 448*, 828−831.

(16) Doi, N., Kumadaki, S., Oishi, Y., Matsumura, N., and Yanagawa, H. (2004) In vitro selection of restriction endonucleases by in vitro compartmentalization. *Nucleic Acids Res. 32*, e95.

(17) Cohen, H. M., Tawfik, D. S., and Griffiths, A. D. (2004) Altering the sequence specificity of HaeIII methyltransferase by directed evolution using in vitro compartmentalization. *Protein Eng., Des. Sel. 17*, 3−11.

(18) Fernandez-Gacio, A., Uguen, M., and Fastrez, J. (2003) Phage display as a tool for the directed evolution of enzymes. *Trends Biotechnol. 21*, 408−414.

(19) Leemhuis, H., Stein, V., Griffiths, A. D., and Hollfelder, F. (2005) New genotype-phenotype linkages for directed evolution of functional proteins. *Curr. Opin. Struct. Biol. 15*, 472−478.

(20) Chen, I., Dorr, B. M., and Liu, D. R. (2011) A general strategy for the evolution of bond-forming enzymes using yeast display. *Proc. Natl. Acad. Sci. U.S.A. 108*, 11399−11404.

(21) Agresti, J. J., Antipov, E., Abate, A. R., Ahn, K., Rowat, A. C., Baret, J. C., Marquez, M., Klibanov, A. M., Griffiths, A. D., and Weitz, D. A. (2010) Ultrahigh-throughput screening in drop-based microfluidics for directed evolution. *Proc. Natl. Acad. Sci. U.S.A. 107*, 4004−4009.

(22) Varadarajan, N., Rodriguez, S., Hwang, B. Y., Georgiou, G., and Iverson, B. L. (2008) Highly active and selective endopeptidases with programmed substrate specificities. *Nat. Chem. Biol. 4*, 290−294.

(23) Colby, D. W., Kellogg, B. A., Graff, C. P., Yeung, Y. A., Swers, J. S., and Wittrup, K. D. (2004) Engineering antibody affinity by yeast surface display. *Methods Enzymol. 388*, 348−358.

(24) Jones, R. P., and Greenfield, P. F. (1987) Ethanol and the fluidity of the yeast plasma membrane. *Yeast 3*, 223−232.

(25) Fujiwara, K., Maita, N., Hosaka, H., Okamura-Ikeda, K., Nakagawa, A., and Taniguchi, H. (2010) Global conformational change associated with the two-step reaction catalyzed by *Escherichia coli* lipoate-protein ligase A. *J. Biol. Chem. 285*, 9971−9980.

(26) Fujiwara, K., Toma, S., Okamura-Ikeda, K., Motokawa, Y., Nakagawa, A., and Taniguchi, H. (2005) Crystal structure of lipoate-protein ligase A from *Escherichia coli*. Determination of the lipoic acid-binding site. *J. Biol. Chem. 280*, 33645−33651.

(27) Scheiffele, P., Fan, J., Choih, J., Fetter, R., and Serafini, T. (2000) Neuroligin expressed in nonneuronal cells triggers presynaptic development in contacting axons. *Cell 101*, 657−669.

(28) Graff, J. M., Stumpo, D. J., and Blackshear, P. J. (1989) Molecular cloning, sequence, and expression of a cDNA encoding the chicken myristoylated alanine-rich C kinase substrate (MARCKS). *Mol. Endocrinol. 3*, 1903−1906.

(29) Craig, A. M., and Kang, Y. (2007) Neurexin-neuroligin signaling in synapse development. *Curr. Opin. Neurobiol. 17*, 43−52.

(30) Chen, S. X., Tari, P. K., She, K., and Haas, K. (2010) Neurexin-neuroligin cell adhesion complexes contribute to synaptotropic dendritogenesis via growth stabilization mechanisms in vivo. *Neuron 67*, 967−983.

(31) Liu, D. S., Loh, K. H., Lam, S. S., White, K. A., and Ting, A. Y. (2013) Imaging Trans-Cellular Neurexin-Neuroligin Interactions by Enzymatic Probe Ligation. *PLoS One 8*, e52823.

(32) Yamagata, M., and Sanes, J. R. (2012) Transgenic strategy for identifying synaptic connections in mice by fluorescence complementation (GRASP). *Front. Mol. Neurosci. 5*, 18.

(33) Kim, J., Zhao, T., Petralia, R. S., Yu, Y., Peng, H., Myers, E., and Magee, J. C. (2012) mGRASP enables mapping mammalian synaptic connectivity with light microscopy. *Nat. Methods 9*, 96−102.
(34) Lin, Y., Tsumuraya, T., Wakabayashi, T., Shiraga, S., Fujii, I., Kondo, A., and Ueda, M. (2003) Display of a functional hetero-oligomeric catalytic antibody on the yeast cell surface. *Appl. Microbiol. Biotechnol. 62*, 226−232.
(35) Gautier, A., Juillerat, A., Heinis, C., Correa, I. R., Jr., Kindermann, M., Beaufils, F., and Johnsson, K. (2008) An engineered protein tag for multiprotein labeling in living cells. *Chem. Biol. 15*, 128−136.
(36) Los, G. V., Encell, L. P., McDougall, M. G., Hartzell, D. D., Karassina, N., Zimprich, C., Wood, M. G., Learish, R., Ohana, R. F., Urh, M., Simpson, D., Mendez, J., Zimmerman, K., Otto, P., Vidugiris, G., Zhu, J., Darzins, A., Klaubert, D. H., Bulleit, R. F., and Wood, K. V. (2008) HaloTag: A novel protein labeling technology for cell imaging and protein analysis. *ACS Chem. Biol. 3*, 373−382.